Deformation of the South American Crust Estimated from Finite Element and Collocation Methods

Hermann Drewes
Deutsches Geodätisches Forschungsinstitut (DGFI), Marstallplatz 8, 80539 München, Germany
e-mail: drewes@dgfi.badw.de

Oliver Heidbach
Geophysical Institute, Karlsruhe University, Hertzstr. 16, 76187 Karlsruhe, Germany
e-mail: oliver.heidbach@gpi.uni-karlsruhe.de

Abstract. The present-day surface velocity field of the South American continent reflects the recent geodynamic features. It varies from quasi rigid body motion in the eastern part to mountain range deformation in the western Andes. Space geodetic observations provide velocities at discrete points only. To represent the continuous velocity field, an adequate deformation model has to be developed. Two different models are applied, the least squares collocation approach (LSC) and the finite element method (FEM). The input data are given by 329 velocities derived from continuously observing GPS stations and several GPS geodynamics projects. The different data sets are transformed to a common kinematic datum by deriving the rotation vector of the South American plate from station motions of the IGS Regional Network (RNAAC-SIR) in the rigid eastern part and reducing these plate motions from all the data sets. The resulting residual motions define the boundary conditions in the FEM and the input signals in the LSC. For the FEM a network of approximately 75000 linear elements is generated. The model rheology is a homogeneous elastic material (Young's modulus 70 GPa and Poisson ratio 0,3). For the LSC empirical covariance functions are derived from the observed velocity vectors. The comparison of both methods shows an agreement in the mm/a level. The result is a continuous surface velocity model for the South American continent which may be used for interpolation of point motions in geodetic networks and reference frames. A detailed geodynamic interpretation has not yet been done due to the simplicity of the model (homogeneous material, rough fault structures, no sophisticated dynamics).

Keywords. Recent crustal movements, South America, SIRGAS, GPS velocity field, collocation, finite element method

1 Introduction

The deformation process of the South American continent is mainly controlled through the push of the Mid Atlantic Ridge from the east, the subduction of the Nazca plate along the Pacific coast in the west and the subduction of the Caribbean plate in the north (fig. 1).

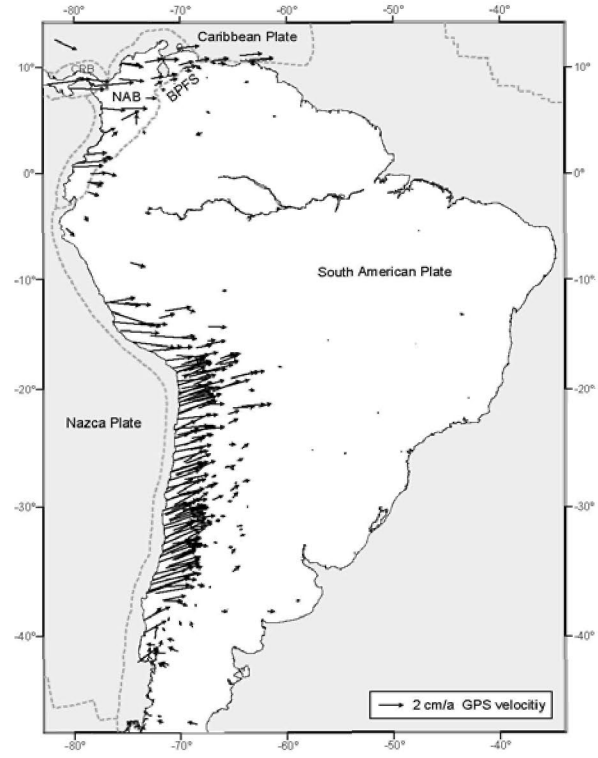

Fig.1: Velocities relative to the stable part of South America derived from different GPS projects (see text). Plate boundaries are taken from (Bird, 2003). NAB = North Andes Block, BPFS = Boconó-El Pilar fault system CRB = Costa Rica Block.

The North Andes Block in the north-western part of the continent (Audemard and Audemard, 2002; Kellogg et al., 1995) is bounded to the south by the dextral shear along the Boconó-El Pilar fault system. As a result the present-day velocity field, as observed by space geodetic techniques, shows a strong variation from east to west (fig. 1).

Dislocation models based on the boundary element method show that the interface between the subducting Nazca plate and the overriding South America plate is locked (Bevis et al., 2001; Khazaradze and Klotz, 2003). Therefore, the movement of the GPS stations in magnitude and direction is mainly due to the relative movement of the Nazca plate with respect to the stable part of the South America plate. This relative movement of the Nazca plate has a present velocity of 65 mm/a with an azimuth of N77°E at 30°S (Angermann et al., 1999). The dislocation modelling results (Bevis et al., 2001; Khazaradze and Klotz, 2003) show that most of the observed inter-seismic velocity field can be explained by that transmission of deformation. The velocity is decreasing perpendicularly to the trench and comes close to zero east of the Sub-Andes where the stable part of the South America plate begins.

In the northern part of the South American plate the situation is more complex. Here the north-west striking and south-east dipping subduction of the Caribbean plate and the collision of the Costa-Rica block influence the deformation of the subduction process described above (Audemard and Audemard, 2002; Kellogg et al., 1995). As a result the North Andes block has been developed. This block moves along a transpressive dextral strike-slip fault system in eastern direction with 10-20 mm/a (Kaniuth et al., 1999).

The South American Geocentric Reference System, SIRGAS (Hoyer et al., 1997; Drewes et al., 2000) defines the station coordinates at a fixed epoch (1995.4 or 2000.4, respectively). To reduce the coordinates determined at another epoch to the reference epoch, the station velocities are needed (Drewes et al., 1997). These may be derived for the SIRGAS stations from repeated observations (1995 and 2000). For new stations, e.g., in the national reference frames, a continuous velocity field is needed to interpolate the required velocities.

2 Used Data Sets and Reductions

Point velocities in South America are available from the following data sets of GPS observations: The IGS Regional Network Associate Analysis Centre for SIRGAS, RNAAC-SIR (Seemüller et al. 2002), the SIRGAS campaigns 1995 and 2000 (Luz et al., 2000, Drewes et al. 2004), the Central and South America geodynamics project, CASA (Kaniuth et al., 1999), the South America - Nazca Plate Motion Project, SNAPP (Norabuena et al., 1998), the Central Andes Project, CAP (Brooks et al.. 2003, Kendrick et al., 1999; Kendrick et al., 2001, Lamb 2000) and the South America Geodynamic Activities, SAGA (Khazaradze and Klotz, 2003; Klotz et al., 2001).

In a first step, the rotation pole of the rigid South American plate was estimated from the velocities of the RNAAC-SIR stations in the stable western continent. The RNAAC-SIR velocities, originally referring to the ITRF 2000 reference frame, were reduced by the plate velocities resulting thus in velocities relative to the rigid South American plate.

In the second step, the velocities of the non-continuously observing SIRGAS stations were derived from the coordinates of the SIRGAS 1995 (transformed from the original ITRF94 to ITRF 2000) and the SIRGAS 2000 (given in ITRF 2000) campaigns. These velocities were then transformed to the RNAAC datum by identical stations.

In the following steps, the velocities of all the geodynamics projects were transformed from their individual kinematic datums (in general relative to an arbitrarily defined stable South America) to the RNAAC datum by identical stations.

The accuracy of observed velocities is in general in the order of some millimeters per year (mm/a). Observations at stations affected by earthquakes were neglected, i.e., only data which reflect the inter-seismic velocity field were taken into account.

3 Modelling of the Velocity Field

To model the velocity field we applied two different methods: the least squares collocation approach and the finite element method. The first one is a mathematical vector prediction algorithm without any geophysical models. It interpolates the velocity field from the discrete observations. The second method uses a simple geophysical model of plate tectonics with an deformable elastic material.

3.1 Finite Element Model

The **V**elocity **M**odel of **S**outh America (VEMOS) from the finite element approach consists of 75000 linear 3D-elements on a sphere with a constant radius of 6371 km. The equation of equilibrium is solved for simple homogeneous linear elastic rheology. The Young module was set to 70 GPa and the Poisson number is 0,3. In the north, the Boconó-El-Pilar fault system which marks the southern border of the North Andes block is implemented as a contact surface where relative sliding is allowed.

The coefficient of friction is set to 0,1. At the northern (20°N) and southern (55°S) boundaries sliding in west-east direction is allowed, the western boundary (-90°W) is free of conditions and the eastern boundary (-34°W) is fixed. The bottom of the model at 10 km depth is fixed in the vertical direction; the surface of the model is free (fig.2). Further boundary conditions are the horizontal components of the given 329 GPS velocities (fig.1).

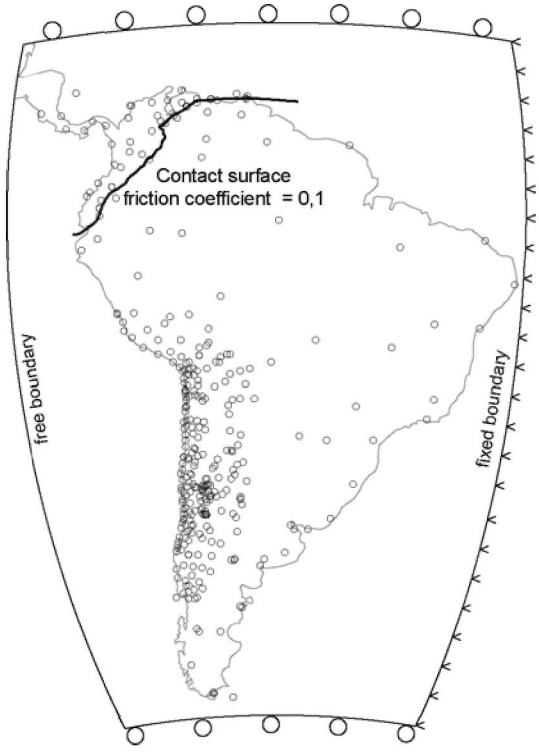

Fig.2: Boundary conditions for the finite element model: The northern and southern boundary condition allows east-west sliding and the eastern boundary is fixed. The bottom of the model at 10 km depth is fixed in vertical direction; the surface of the model is free. The Boconó-El-Pilar fault system (grey line) is modelled as a contact surface where relative sliding is allowed. The circles are the locations of the GPS observation points.

3.2 Least Squares Collocation

The least squares collocation approach uses the well-known relation between correlated signals:

$$\mathbf{v}_{pred} = \mathbf{c}_{in}^{T}\, \mathbf{C}_{ij}^{-1}\, \mathbf{v}_{obs}$$

$\mathbf{v}_{obs}$ are the observed and $\mathbf{v}_{pred}$ the predicted point velocity vectors, $\mathbf{C}_{ij}$ is the auto-covariance matrix between the observed and $\mathbf{c}_{in}$ the cross-covariance matrix between the observed and the predicted velocity vectors.

The elements of the covariance matrices are taken from empirically determined isotropic covariance functions, each one for the north and east velocity components and one for the cross correlation between north and east components. The empirical correlations are computed in distance (d) classes between the points and approximated by a simple exponential function: $a \cdot \exp(-b \cdot d)$. To get a sufficiently dense input velocity field, a wide-spaced grid is interpolated linearly in areas with sparse observations, in particular in the central part of the continent (Amazon region).

The prediction error of velocities is typically in the order of the observation errors, i.e., some mm/a.

4 Results

4.1 Finite Element Model

The results of the finite element model (fig. 3) can be distinguished in four first order patterns:
(1) The high gradient of the velocity field across the dextral Boconó-El-Pilar fault system in the north-west of the continent. This gradient decreases from east to south-west due to increasing transpressional

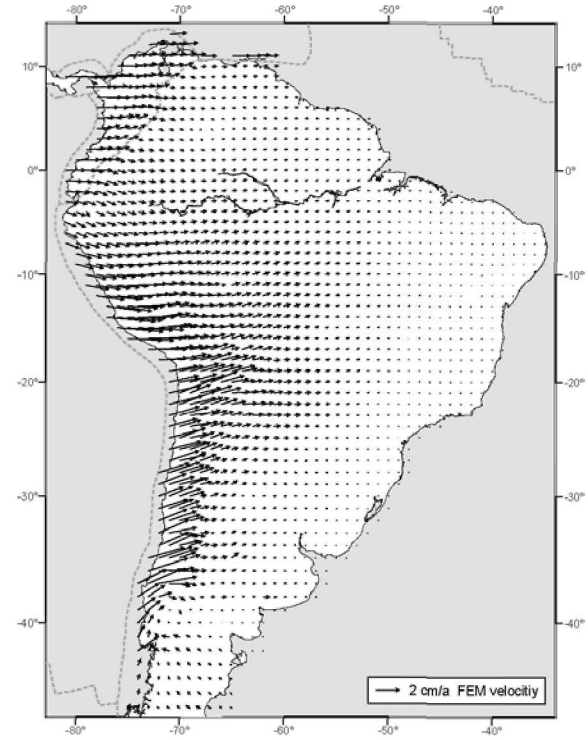

Fig.3: Horizontal velocity field from the finite element model with a Young module of 70 GPa and a Poisson number of 0,3. The coefficient of friction at the Boconó-El-Pilar fault system is set to 0,1. Boundary conditions at the model border and the GPS data are presented in the previous figures.

(2) The area between the equatorial region and 25° southern latitude where the velocity field decreases smoothly east of the Sub-Andes. The decrease is nearly linear from west to east and becomes zero at the Atlantic coast
(3) The area between 25°S and 38°S where the velocity field decreases east of the eastern cordillera and trends then smoothly to zero at the Atlantic coast.
(4) The area south of 37°S where the few observed velocity vectors do not show a clear picture and therefore the velocity field is not quite significant.

4.2 Least Squares Collocation

The result of the collocation approach (fig. 4) shows naturally in principle the same four mentioned patterns, but it deviates slightly in pattern (2). Here the decrease is stronger than in the finite element model. This may be due to the steep covariance function in this region which is characteristic for short correlation lengths between the velocities. For this reason the large velocities in the Andean deformation zone are not transferred to the central part of the continent. That means, that we have a relatively sharp separation between deformation zone and rigid plate.

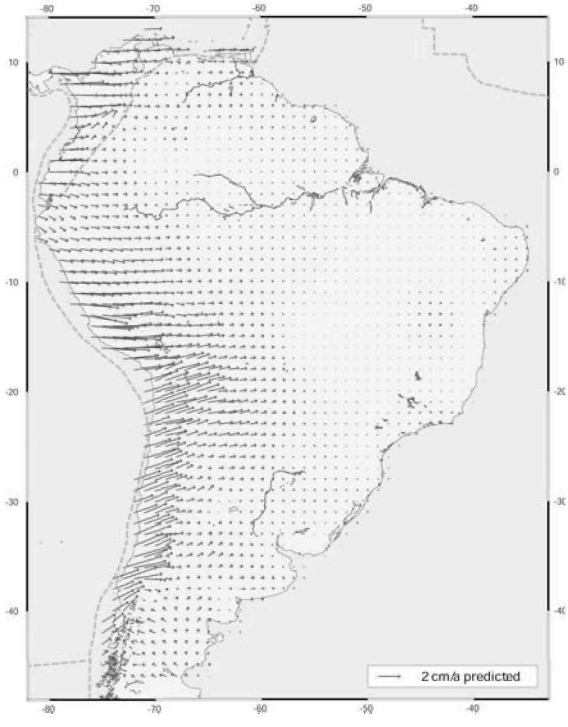

Fig.4: Horizontal velocity field from the least squares collocation (vector prediction) approach with empirically determined covariance functions.

5 Comparison

The numerical comparison of the two approaches shows a general good agreement. The numbers are:

Average difference West-East:	– 1.0 mm/a
Average difference South-North	– 0.1 mm/a
r.m.s. difference West-East:	± 1.7 mm/a
r.m.s. difference South-North:	± 0.9 mm/a.

The main systematic deviations between both models are generated by the smooth (FEM) or steep (LSC) transition from the Andean deformation zone to the rigid region in the central continent. The differences come up to a maximum of 7 mm/a in West-East and 5 mm/a in South-North direction. This phenomenon has further to be investigated, in particular with respect to the elasticity parameters and the covariance functions.

6 Discussion

The result of this research project is a continuous surface velocity model for the South American continent which may be used for interpolation of point motions in geodetic networks and reference frames. The long-term problem is that the used data sets only reflect the inter-seismic signals, i.e., in regions where major earthquakes occur the reduction of coordinates cannot be done with linear velocities since the co- and post-seismic signal changes the velocity field in a wide area (Angermann et al., 2003; Kaniuth et al., 2002; Pollitz et al., 2000). Since all the GPS stations in the western part of the continent close to the Nazca subduction will sooner or later be affected by earthquakes, the velocity models are only a first approximation.

Also the effects of further major strike slip and thrust faults in the Andes were neglected and are probably not accurately reflected in the GPS data. For future demands, either from scientific curiosity or from geodesy, on higher resolutions in time and space the finite element approach seems to be the better option than the collocation approach. The simple kinematic model with homogeneous elastic material, only rough fault structures and no sophisticated dynamics, however, has to be improved and to be extended to a complete three-dimensional dynamic viscous-elastic-plastic model with detailed tectonic structures (e.g. Heidbach and Drewes, 2003). The more GPS data become available the more we will learn on relative movements along active faults or rigid blocks which move along major fault systems. In the present study we did not accomplish a detailed geodynamic interpretation due to the simplicity of the models.

7 Conclusion

We conclude three statements:
(1) More observations in space and time are needed to isolate the linear from the non-linear part of the observed signals. There are observation gaps, e.g., between 0° and 10°S and in southern Chile,
(2) For more accurate application of the velocity field the influence of the viscous relaxation processes in return of the earthquakes must be investigated, and
(3) More neotectonic structures and a more sophisticated rheology to account for the relaxation processes has to be applied in a more detailed model which incorporates, e.g., thrust faults of the Sub-Andes (Norabuena et al., 1998) and inhomogeneous and layered rheolgy (Wdowinski and Bock, 1994).

8 References

Angermann D., Klotz J., Reigber C. (1999) Space-geodetic estimation of the Nazca-South America Euler vector. *Earth Planet Sc Lett.* **171**, 329-334.

Angermann D., Krügel M., Meisel B., Müller H., Tesmer V. (2003) Time series of station positions and datum parameters. *Geotechnologien Science Report* **No. 3,** 17-21.

Audemard F.E., Audemard F.A. (2002) Structure of the Mérida Andes, Venezuela: relations with the South America-Caribbean geodynamic interaction. *Tectonophysics* **345**, 299-327.

Bevis M., Kendrick E., Smalley J.R., Brooks B., Allmendinger R., Isacks B. (2001) On the strength of interplate coupling and the rate of back arc convergence in the central Andes: An analysis of the interseismic velocity field. *Geochem., Geophys., Geosyst.* **2**, 10.1029/2001GC000198.

Bird P. (2003) An updated digital model for plate boundaries. *Geochem., Geophys., Geosyst.* **4** (3), 1027, doi: 10.1029/2001GC000252.

Brooks, B.A., Bevis, M., Smalley, J.R., Kendrik, E., Manceda, R., Lauría, E., Maturana, R., Araujo, M. (2003) Do the Andes behave like a microplate? *G^3 Geochem., Geophys., Geosyst.* **4**, (10), 1085, doi: 10.1029/2003GC000505.

Drewes H. (1997) Time evolution of the SIRGAS reference frame. *IAG Symposia* **118,** 174-179, Springer, Berlin.

Drewes H., Kaniuth K., Seemüller W., Stuber K., Tremel H., Hernandez N., Hoyer M., Wildermann E., Fortes L.P., Pereira K.D. (2000) Monitoring the Continental Reference Frame in South America. *IAG Symposia* **124**, 134-137. Springer, Berlin.

Drewes, H., Kaniuth, K., Völksen, C., Costa, S.M., Fortes, L.P. (2004) Results of the SIRGAS Campaign 2000 and coordinates variations with respect to the 1995 South American Geocentric Reference Frame. *IAG Symposia* (this volume) Springer, Berlin.

Heidbach, O., Drewes, H. (2003) 3-D Finite Element model of major tectonic processes in the Eastern Mediterranean. In: Nieuwland, D.A. (ed.) New insigths in structural interpretation and modelling, *Geological Society, Spec. Pub.* **212**, 261-274, London.

Hoyer, M., Arciniegas, S., Pereira, K., Fagard, H., Maturana, R., Torchetti, R., Drewes, H., Kumar, M., Seeber, G. (1997) The definition and realization of the reference system in the SIRGAS project. *IAG Symposia* **118,** 168-173, Springer, Berlin.

Kaniuth K., Drewes H., Stuber K., Tremel H., Hernández N., Hoyer M., Wildermann E., Kahle H. G., Geiger A., Straub C. (1999) Position changes due to recent crustal deformations along the Caribbean - South American plate boundary derived from the CASA GPS Project. *XXII IUGG General Assembly*, Birmingham, UK.

Kaniuth K., Müller H., Seemüller W. (2002) Displacement of the space geodetic observatory Arequipa due to recent earthquakes. *Zeitschr. für Verm.* **127**(4), 238-243.

Kellogg J.N., Vega V., Stallings T.C., Aiken C. L.V. (1995) Tectonic development of Panama, Costa Rica, and the Colombian Andes: Constraints from Global Positioning System geodetic studies and gravity. In: Mann, P. (ed.) Geologic and Tectonic Development of the Caribbean Plate Boundary in Southern Central America, *Geol. Soc. Am. Special Paper* **295,** 75-90.

Kendrick E., Bevis M., Smalley J.R., Brooks B. (2001) An integrated crustal velocity field for the central Andes. *Geochem. Geophys. Geosyst.* **2**, 10.129/2001GC000191.

Kendrick E.C., Bevis M., Cifuentes O., Galban F. (1999) Current rates from convergence across the Central Andes: Estimates from continuous GPS observations. *Geophys. Res. Lett.* **26**(5), 541-544.

Khazaradze G., Klotz J. (2003) Short- and long-term effects of GPS measured crustal deformation rates along the south central Andes. *J. Geophys. Res.* **108** (B6), 2289, doi: 10.1029/2002JB001879.

Klotz J., Khazaradze G., Angermann D., Reigber C., Perdomo R., Cifuentes, O. (2001) Earthquake cycle dominates contemporary crustal deformation in Central and Southern Andes. pp. 437-446.

Lamb S. (2000) Active deformation in the Bolivian Andes, South America. *J. Geophys. Res.* **105**, 25627-25653.

Luz, R.T., Fortes, L.P., Hoyer, M., Drewes, H. (2002) The vertical reference frame for the Americas – The SIRGAS 2000 GPS campaign. *IAG Symposia* **124**, 302-305. Springer, Berlin.

Meijer P.T. and Wortel M.J.R. (1997) Present-day dynamics of the Agean region: A model analysis ot the horizontal pattern of stress and deformation. *Tectonics* **16**, 879-895.

Norabuena,E., L. Leffler-Griffin; A. Mao; T. Dixon; S. Stein; I.S. Sacks; L. Ocola; M. Ellis (1998): Space geodetic observations of Nazca-South America convergence across the Central Andes. *Science* (279) 358-362.

Pollitz F. F., Peltzer G. and Bürgmann R. (2000) Mobility of continental mantle: Evidence from postseismic geodetic observations following the 1992 Landers earthquake. *J. Geophys. Res.* **105**, 8035-8054.

Seemüller, W., Kaniuth, K., Drewes, H. (2002) Velocity estimates of IGS RNAAC SIRGAS stations. *IAG Symposia* **124**, 7-10. Springer, Berlin.

Wdowinski S. and Bock Y. (1994) The evolution of deformation and topography of high elevated plateaus: 2. Application to the central Andes. *J. Geophys. Res.* **99**, 7121-7130.